DEUTSCHES ELEKTRONEN-SYNCHROTRON DESY

DESY 67/21
September 1967

NEUTRON FORM FACTORS FROM ANALYSIS OF DEUTERON ELECTRODISINTEGRATION EXPERIMENTS

By

D. Hasselmann and G. Kramer

Physikalisches Staatsinstitut
II. Institut für Experimentalphysik, Hamburg

2 HAMBURG 52 · NOTKESTIEG 1

NEUTRON FORM FACTORS FROM ANALYSIS OF DEUTERON ELECTRODISINTEGRATION EXPERIMENTS

By

D. Hasselmann and G. Kramer

Physikalisches Staatsinstitut
II. Institut für Experimentalphysik, Hamburg

Abstract

Electromagnetic form factors of the neutron are calculated from recent quasi-elastic electron-deuteron scattering experiments done at Orsay and Stanford. The theory used in the analysis includes a realistic description of the deuteron and rescattering corrections.

Introduction

Recently we presented, together with D. Braess[1], the results of an analysis of an inelastic electron-deuteron scattering experiment done by Hughes, Griffy, Yearian and Hofstadter at Stanford[2]. In this experiment only the scattered electron was detected and the electron-deuteron cross section at the quasi-elastic peak was measured with high accuracy. Our analysis was restricted to the data with momentum transfers q^2 below 5 f^{-2}, since in this range of q^2 final state interaction effects are important. The Stanford measurements were made up to q^2 = 35 f^{-2}. Therefore, we find it worthwhile to extend our analysis in order to have results for neutron form factors in the q^2 range from q^2 = 1 f^{-2} up to q^2 around 30 f^{-2} based on the theoretical picture which was developed by D. Braess and one of us[3]. The experimental data in ref. 2 have already been analysed towards neutron form factors by the experimenters using Durand's simple theory[4] supplemented by rescattering corrections extrapolated from the theoretical work of Nuttall and Whippman[5] and a deuteron-pole term contribution. Unfortunately, it is doubtful whether this deuteron-pole term should be added since this contribution should be contained in the final-state interaction correction. Since for the higher q^2 the rescattering corrections and the deuteron-pole contribution seem to be small[2] we do not expect very different neutron form factors above q^2 = 10 f^{-2} compared to the results obtained in ref. 2. So our emphasis is more on the application of a uniform theory to the analysis of the high accuracy quasi-elastic electron-deuteron scattering data for all q^2 up to f^{-2}.

Besides the Stanford data we analyse some recent measurements of the Orsay group around q^2 = 3.5 f^{-2} [6] which have been also analysed already by the experimenters[6] and by Bosco, Grossetête and Quarati[7]. We think that the theoretical description of the deuteron electro-disintegration process at the quasi-elastic peak as presented in ref.3 is superior to the description used by these two groups.

Unfortunately, we are not able to treat recent data from inelastic electron-deuteron scattering experiments where the outgoing electron and one of the nucleons have been detected in coincidence[8]. Before doing this case we would like to know several corrections to the simple nucleon-pole approximation. Our theory in ref. 3 was only pursued up to the end for noncoincidence measurements.'

In Section II we collect some formulas which are the basis of our analysis. Section III contains the results.

II. Theoretical Preliminaries

In accordance with (II) the cross section for the process e+d→e+p+n is written in the following way:

$$\frac{d^2\sigma}{d\Omega dE'} = \sigma_{Mott} \frac{m^2 p}{\pi\sqrt{m^2 + p^2}} \quad I(\theta,E') \tag{1}$$

with

$$\sigma_{Mott} = \frac{\alpha^2}{4E^2} \frac{\cos^2\theta/2}{\sin^4\theta/2} \tag{2}$$

The notation is as in (I), E and E' are the laboratory energies of the initial and final electron, θ is the electron scattering angle in the laboratory system. m is the nucleon mass and p the momentum of the outgoing proton or neutron in the c.m.-system. In the one-photon exchange approximation the function $I(\theta,E')$ is linear in $\tan^2 \delta/2$ with coefficients which can be expressed by the longitudinal part $I_l = I_l(E')$ and transversal part $I_t = I_t(E')$ of the cross section in the following form (see eq. (II,4) and eq. (II,9))[9]

$$I(\theta,E') = I_l(E') + I_t(E')\cdot y \tag{3}$$

with

$$y = \frac{q^2}{4m^2} (1 + (1 + q^2/4m^2)\ 2 \tan^2 \theta/2) \tag{4}$$

q^2 is the invariant square of the momentum transfer q and $q^2 = \vec{q}^2 - q_o^2$.

The longitudinal and transversal parts of the cross section depend on the proton form factors G_{1E} and G_{1M} and the neutron form factors G_{2E} and G_{2M}. For the theory developed in (I) this dependence is as follows (see eq. (II,8))

$$I_l = (G_{1E}^2 + G_{2E}^2) A_l + 2 G_{1E} G_{2E} B_l \tag{5}$$

$$I_t = (G_{1M}^2 + G_{2M}^2) A_t + 2 G_{1M} G_{2M} B_t + (G_{1E}^2 + G_{2E}^2) C_t$$

$$+ 2 G_{1E} G_{2E} D_t + 2(G_{1E} G_{1M} + G_{2E} G_{2M}) E_t$$

$$+ 2 (G_{1E} G_{2M} + G_{2E} G_{1M}) F_t .$$

The coefficients A_l, B_l, A_t, B_t etc. are determined by the theory. Similar to the cases with $q^2 < 5\ f^{-2}$ already treated in (II) we find also for the higher q^2 that C_t, D_t, E_t and F_t are completely negligible compared to A_t and B_t. The numerical results of the remaining coefficients A_l, B_l, A_t and B_t are collected for possible further application in Table 1 but only for the q^2 needed to analyse the experimental data of ref. 6 and ref. 2. The momentum transfer q^2 for the quasi-elastic e-d scattering differ slightly from the momentum transfer of the corresponding elastic e-p scattering. The q^2 for the e-p scattering measurements at Stanford were q^2 = 7.5, 10.0, 12.5, 15.0, 20.0, 25.0, 30.0 and 35.0 measured in f^{-2} which are used later on to refer to the corresponding quasi-elastic e-d data in particular in all tables except Table 1.

III. Analysis and Results

A. Orsay Measurements

We start with the analysis of the Orsay data[6]. Grossetête, Jullian and Lehmann measured with an accuracy of roughly 4 % the cross section $d^2\sigma/d\Omega dE'$ for two scattering angles $\theta = 60^o$ and $\theta = 130^o$ and five incident electron energies E at the quasi-elastic peak. Their results together with the parameters which are of interest to us are given in Table 2. From these data we calculated $I(\delta,E')$ according to formula (1). Since the two measurements around $q^2 = 2.9\ f^{-2}$ for $\theta = 60^o$ and $\theta = 130^o$ do not yield the same q^2. we interpolated $I(\theta,E')$ for $q^2 = 2.9\ f^{-2}$ from the three data available for $\theta = 60^o$. Then the empirical values vor I_l and I_t are determined by a least-squares fit of the relation (3) to the data. The results of this fit are exhibited in Table 3 together with the proton form factor G_{1E} and G_{1M} needed for further analysis. The proton form factors are calculated from a three parameter interpolation formula constructed in (II). Now the computation of G_{2E} and G_{2M} is straightforward.

G_{2E} is obtained from eq. (II,4):

$$G_{2E} = G_{1E} \left(- \frac{B_1}{A_1} \pm \sqrt{\frac{I_1}{G_{1E}^2 A_1} + \left(\frac{B_1}{A_1}\right)^2 - 1} \right) \qquad (6)$$

Unfortunately, it is not quite clear which sign in front of the aquare root in formula (6) should be attributed to the physical G_{2E}.

In (II) we decided for the negative sign to have a smooth variation of G_{2E} with q^2 taking into account that the slope of G_{2E} at $q^2 = 0$ has a value around $0.02\ f^2$ as measured in neutron-electron scattering experiments. With this sign we obtain the values labelled $G_{2E}^{(-)}$ in Table 3. For later comparison also the values with the positive square root, labelled $G_{2E}^{(+)}$ in Table 3, are shown. In every column for G_{2E} in Table 3 three values are given, the upper and lower numbers are upper and lower bounds where only the uncertainty from I_1 is included but not the uncertainty from the empirical proton form factors.

G_{2M} is calculated from eq. (II,16)

$$G_{2M} = G_{1M} \left(- \frac{B_t}{A_t} - \sqrt{\frac{I_t}{G_{1M}^2 A_t} - 1 + \left(\frac{B_t}{A_t}\right)^2} \right) \tag{7}$$

Here no ambiguity concerning the sign of the square root exists since we do not expect G_{2M} to change sign in the q^2 range considered. The result of our calculation for $G_{2M/\mu 2}$ is also shown in Table 3 ($\mu 2 = -1.913$)

B. Stanford Measurements

Hughes et al.[2)] have presented their experimental e-d scattering results in terms of R_o, the corrected ratio of the elastic electron-proton cross section to the quasi-elastic electron-deuteron cross section. Then I (θ, E') must be calculated from R_o with the formula (see eq. (II,11)):

$$I(\theta,E') = \pi \frac{\sqrt{p^2+m^2}}{m^2 p} \frac{G_p(\theta, q^2)}{1 + \frac{2E}{m}\sin^2\theta/2} \frac{1}{R_o} \tag{8}$$

where $G_p(\theta,q^2)$ is the elastic electron-proton scattering cross section divided by the nuclear cross section (see eq.(II,12)). To evaluate $I(\theta,E')$ according to eq.(8) we need the proton form factor at exactly the same q^2 for which R_o was measured. For this purpose we consider the three-pole-fit of Jannssens, Hofstadter, Hughes and Yearian[(10)] as a good interpolation formula for the proton form factor in the q^2 range we are interested in. The form factors G_{1E} and G_{1M} obtained from this fit were checked against recent analysis of elastic e-p data including measurements from DESY[11)] in such cases where the q^2 coincided.

The agreement, in particular for G_{1M}, is inside 3 %. The influence of slightly different proton form factors on the results for the neutron form factors will be discussed later. The $I(\theta,E')$ computed from the empirical R_o and proton form factors G_{1E} and G_{1M} are fitted to eq. (3) and the longitudinal and transversal cross sections I_l and I_t respectively are determined. The results are given in Table 4. The neutron form factors again follow from eq. (6) and eq. (7). First we consider results for G_{2M/μ_2} shown in Table 5. Compared to the results of the analysis in ref. 2 we obtained somewhat smaller values for G_{2M/μ_2}. The column for G_{2M/μ_2} in Table 5 should be compared with the columns for G_{1E} and G_{1M/μ_1} in Table 4 as a test of the relation $G_{1E} = G_{2M/\mu_2} = G_{1M/\mu_1}$ ($\mu_1 = 2.793$). In Fig. 1 we have collected the data about the ratio $G_{1M/\mu_1}/G_{2M/\mu_2}$ from ref.1 and this analysis. Except for the points in the low q^2 range, the three form factors G_{1E}, G_{1M} and G_{2M} follow rather well the law

$$G_{1M/\mu_1} = G_{2M/\mu_2} = G_{1E}$$

up to $q^2 = 30.0\ f^{-2}$. Furthermore, we remark that the rescattering corrections for G_{2M/μ_2} are not negligible. They produce a change of G_{2M}, compared to the Born approximation values, by maximal 5 %. The correction has its maximum around $q^2 = 15\ f^{-2}$ for the q^2 considered in this analysis. Table 1 shows that the neutron-proton interference is negligible for q^2 above 10 f^{-2}.

Now we come to the analysis towards the electric form factor of the neutron. Here, the situation is as bad as we met it in our analysis of the low q^2 data[1]. Again the experimental values of I_l are such that a rather complete cancellation takes place in the radicand r:

$$r = \frac{I_l}{G_{1E}^2 A_1} - \left(1 - \left(\frac{B_1}{A_1}\right)^2\right) \qquad (9)$$

of the square root in eq.(6). Unfortunately, r is not alway positive even when we take into account the experimental errors of I_l. To see this explicitly we have listed $I_1 - G_{1E}^2 A$ as a function of q^2 in Table 4

$$(\frac{B_1}{A_1})^2 G_{1E}^2 A_1$$

being negligible. For the four higher q^2 this difference is just zero inside the experimental errors of I_1.

For the first three q^2, $I_1 - G_{1E}^2 A_1$ is definitely negative. This failure can lie as well in the application of an incorrect theory as in systematic errors of the experimental data for I_1. A measure for the relative change needed to arrive at $G_{2E} + \frac{B_1}{A_1} G_{1E} \simeq G_{2E} = 0$ is given by the value of r which we exhibit in Table 5. So appreciable changes of I_1 or $G_{1E}^2 A_1$ are necessary to make $r \geq 0$. In the three cases where $r \geq 0$ inside the experimental accuracy we are allowed to give upper and lower limits for G_{2E}, they are shown in Table 5. To see how far the hypothesis $G_{2E} = 0$ is supported by the empirical data we plotted in Fig. 2 $I_1/G_{1E}^2 A_1$ for the measurements at Stanford and Orsay and compare with the theoretical curve $I_1/G_{1E}^2 A_1 = 1$ as a function of q^2. I_1 for $q^2 < 5\ f^{-2}$ has been taken from ref. 1. Any conclusions from this figure will be left to the reader.

Our results, in particular those concerning G_{2E}, are insensitive to changes of the form factors of the proton. We varied G_{1E} and G_{1M} by ± 5 % and in that indeed I_1 and I_t change by the same amount but the radicand r is not altered since it depends on $\frac{I_1}{G_{1E}^2}$ and $\frac{I_t}{G_{1M}^2}$ respectively. So negative r's cannot be cured by assuming that the proton form factors differ from the Stanford three-pole fit.

Table Captions:

Table 1: Coefficients of longitudinal and transversal cross section I_l and I_t.

Table 2: Orsay data around $q^2 = 3.5\ f^{-2}$.

Table 3: I_l and I_t from Orsay data, together with proton and neutron form factors.

Table 4: I_l and I_t from Stanford data and G_{1E} and G_{1M} from Stanford three pole fit.

Table 4: Results for G_{2E} and G_{2M} from analysis of Stanford data.

Figure Captions:

Fig. 1: Comparison of the magnetic form factors of the neutron and proton for $q^2 \leq 30.0\ f^{-2}$.

Fig. 2: Test of the hypothesis $G_{2E} = 0$

References:

1) Braess, D: D. Hasselmann and G. Kramer
DESY 66/21 and Z.Phys. 198, 527 (1967). This paper will be referred to as (II) and formulas of this paper as eq.(II,number)

2) Hughes, E.B.: T.A. Griffy, M.R. Yearian and R. Hofstadter
Phys.Rev. 139, B458 (1965)

3) Braess, D.: and G. Kramer: Z.Physik 189, 242 (1966). This paper will be referred to as (I).

4) Durand, L.III: Phys.Rev.123, 1393 (1961)

5) Nutall, J: and M.L. Whippmann: Phys.Rev. 130, 2498 (1963)

6) Grossetête, B: S.Jullian and P.Lehmann: Phys.Rev.141, B 1435 (1966)

7) Bosco B: B. Grossetête and P. Quarati: Phys. Rev. 141, 1441 (1966)

8) Stein, P: M. Binkley, R.McAllister, A. Suri and W. Woodward:
Phys.Rev.Lett.16, 592 (1966)

9) Unfortunately formula (4) in (II) was written down incorrectly. It must read

$$I(\theta,E') = I_1(E') + I_t(E') \frac{q^2}{4m^2} (1 + q^2/4m^2) \left[\frac{1}{1+q^2/4m^2} + 2 \tan^2 \theta/2\right]$$

Only with this definition of I_t the numerical results in Table 2 of (II) are brought out. Therefore, also y in eq.(10) of (II) must be:

$$y = q^2/4m^2 (1 + 2(1 + q^2/4m^2) \tan^2 \theta/2)$$

Other corrections in (II) (Z.f.Physik 198, 527 (1967)) are:

p.535 ..... In the representation of I_t the coefficients $C_t, D_t \ldots$,

p.536 ..... fit to all measurements of the particular q^2 for I_t:I_t = 112.9 ± 10.5 ...... to be compared with the results in I_t in Table 2.

10) Jannssens, T: R. Hofstadter, E.B. Hughes and M.R. Yearian:
Phys.Rev. 142, B 922 (1966)

11) Bartel, W. B. Dudelzak, H. Krehbiel, J.M. McElroy, U.Meyer-Berkhout, R.J. Morrison, H. Nguyen-Ngoc, W. Schmidt and G. Weber:
Phys.Rev.Lett. 17, 608 (1966).

Albrecht, W., H.J. Behrend, F.W. Brasse, W. Flauger,
H. Hultschig and K.G. Steffen: Phys.Rev.Lett. 17, 1192 (1966)
Behrend, H.J., F.W. Brasse, J. Engler, H. Hultschig,
S. Galster, G. Hartwig, H. Schopper and E. Ganssauge:
DESY 66/27

Table 1

q^2 $[f^{-2}]$	A_l $[f]$	B_l $[f]$	A_t $[f]$	B_t $[f]$
2.917	3.504	-0.2839	3.499	-0.3091
3.790	2.763	-0.1590	2.736	-0.1837
4.115	2.558	-0.1286	2.526	-0.1530
7.496	1.401	-0.0199	1.381	-0.0455
10.01	1.026	-0.0044	1.014	-0.0246
12.44	0.8069	-0.00028	0.7964	-0.0139
14.97	0.6541	+0.0016	0.6443	-0.0075
19.97	0.4690	0.0003	0.4634	-0.0062
24.96	0.3593	-0.0004	0.3552	-0.0049
29.97	0.2868	-0.0007	0.2844	-0.0049
34.94	0.2356	-0.0000	0.2338	-0.0003

Table 2

E [MeV]	θ [deg]	E' [MeV]	q^2 [f^{-2}]	$\frac{d^2\sigma}{d\Omega dE'}$ [10^{-33} cm^2]
363.8	60	302.6	2.829	10.11 ± 3.5 %
219.9	130	157.3	2.908	1.905 ± 3.5 %
426.6	60	345.3	3.786	6.334 ± 3.9 %
447.1	60	356.7	4.099	5.30 ± 3.8 %
268.9	130	180.0	4.089	1.1092 ± 3.1 %

Table 3

2 f^{-2}	f^{I}	$f^{I}t$	G_{1E}	G_{1M/μ_1}	$G_{2E}^{(-)}$	$G_{2E}^{(+)}$	G_{2M/μ_2}	$G_{2M/\mu_2}/G_{1M/\mu_1}$
2.917	1.842 ± 0.162	25.26 ± 1.35	0.7299	0.7255	<0.059	0.266	0.8378	1.15 ± 0.032
					<0.059	>0.059	± 0.023	
					-0.147	>0.059		
4.115	1.19 ± 0.11	13.39 ± 0.63	0.6581	0.6471	<0.033	0.312	0.690	1.07 ± 0.08
					-0.153	0.219	± 0.047	
					-0.246	>0.033		

Table 4

q^2 [f^{-2}]	I_1 [f]	I_t [f]	G_{1E}	G_{1M}/μ_1	$I_1 - G_{1E}^2 A_1$
7.5	0.2985 ± 0.0148	3.689 ± 0.058	0.4941	0.4798	-0.044 ± 0.015
10.0	0.1406 ± 0.0095	1.936 ± 0.033	0.4127	0.4008	-0.034 ± 0.009
12.5	0.07496 ± 0.01102	1.125 ± 0.028	0.3506	0.3426	-0.0242 ± 0.0110
15.0	0.05009 ± 0.009731	0.6840 ± 0.0209	0.3019	0.2965	-0.00952 ± 0.00973
20.0	0.01724 ± 0.00777	0.2874 ± 0.0134	0.2308	0.2301	-0.00774 ± 0.00777
25.0	0.003786 ± 0.01403	0.1539 ± 0.0137	0.1822	0.1847	-0.00814 ± 0.01403
30.0	0.003998 ± 0.01372	0.07394 ± 0.00854	0.1471	0.1522	-0.0022 ± 0.0137

Table 5

q^2 $[f^{-2}]$	G_{2M}/μ_2	r	G_{2E}
7.5	0.468 ± 0.012	-0.128 ± 0.043	-
10.0	0.410 ± 0.011	-0.194 ± 0.055	-
12.5	0.362 ± 0.013	-0.245 ± 0.111	-
15.0	0.316 ± 0.014	-0.162 ± 0.163	0.00 ± 0.01
20.0	0.234 ± 0.016	-0.304 ± 0.310	0.00 ± 0.02
25.0	0.210 ± 0.024	-0.684 ± 1.172	0.00 ± 0.13
30.0	0.144 ± 0.031	-0.357 ± 2.206	0.00 ± 0.20

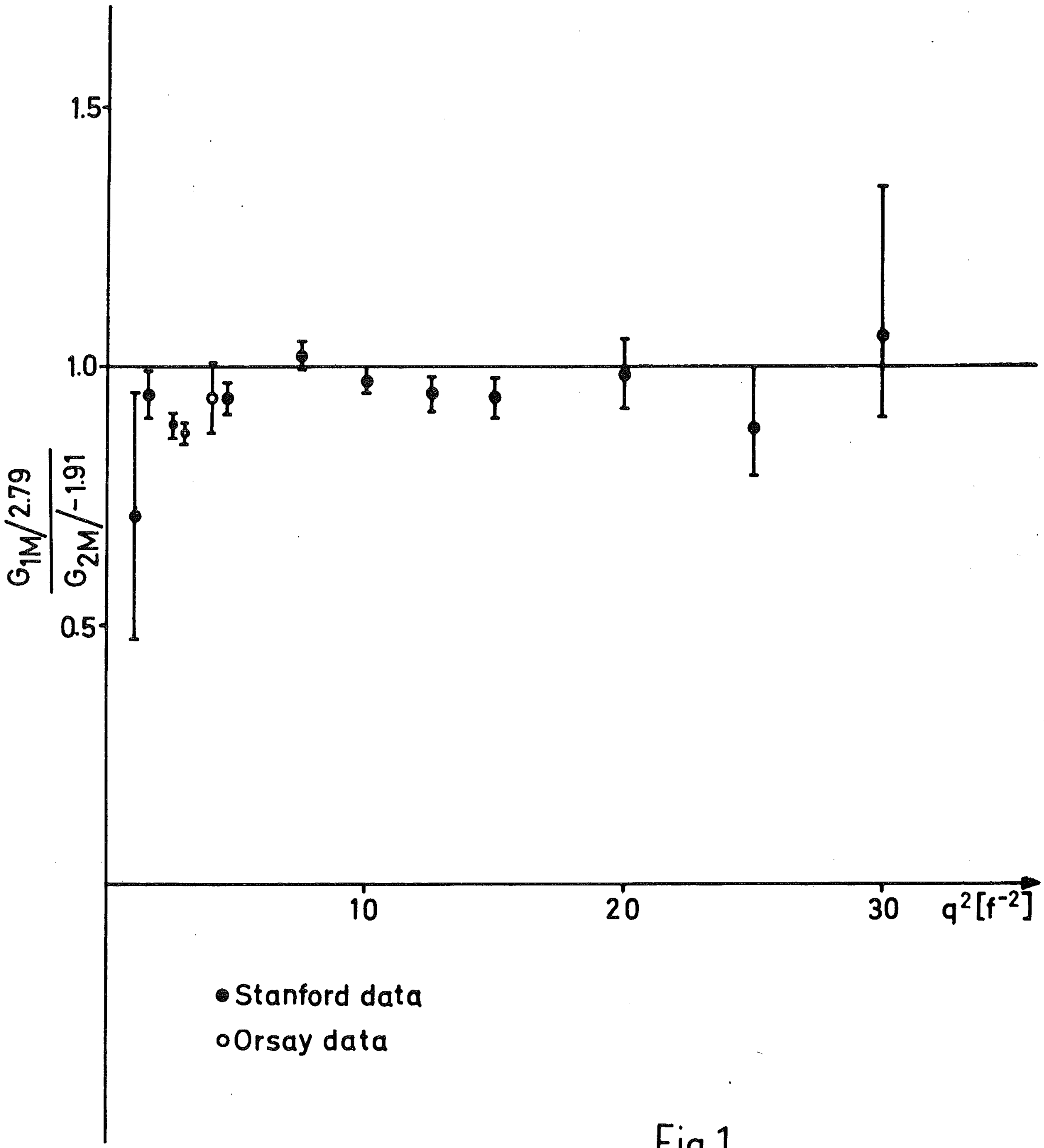
1.5
1.0
0.5
$\frac{G_{1M}/2.79}{G_{2M}/-1.91}$
10
20
30
$q^2\,[f^{-2}]$
● Stanford data
○ Orsay data

Fig. 1

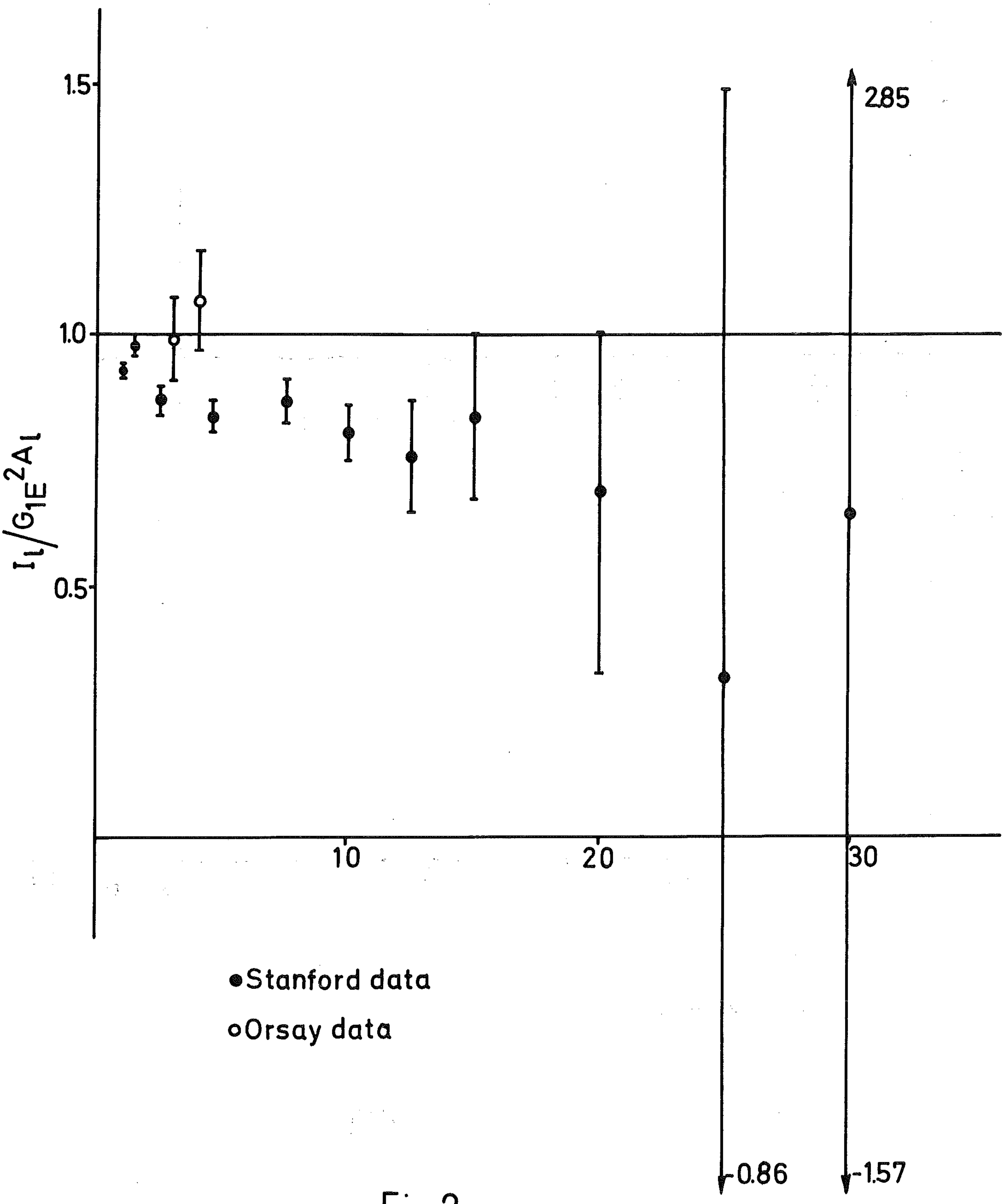
1.5
1.0
0.5
$I_l/G_{1E}{}^2A_l$
10
20
30
2.85
-0.86
-1.57
●Stanford data
○Orsay data

Fig.2